

Measurement of the proton beam energy of a medical cyclotron based on Rutherford Back-scattering Analysis

L. Campajola^{a,b}, S. Braccini^c, P. Casolaro^{a,b,*}, D. de Luca^{a,b}, A. Ereditato^c, P.D. Häffner^c, P. Scampoli^{a,c}

^a Department of Physics “Ettore Pancini”, University of Naples Federico II, Complesso Universitario di Monte S. Angelo, Via Cintia, Napoli, Italy

^b Istituto Nazionale di Fisica Nucleare, Sezione di Napoli, Complesso Universitario di Monte S. Angelo, via Cintia, 80126 Napoli, Italy

^c Albert Einstein Center for Fundamental Physics (AEC), Laboratory for High-Energy Physics (LHEP), University of Bern, Bern 3012, Switzerland

ARTICLE INFO

Keywords:

Beam energy

Medical cyclotron

Rutherford Back-Scattering Spectroscopy (RBS)

ABSTRACT

For the first time the Rutherford Back-Scattering Spectroscopy (RBS) technique has been successfully exploited for the measurement of the energy of a proton beam accelerated by the IBA Cyclone 18/18 medical cyclotron in operation at the Bern University Hospital. This accelerator, routinely used for radioisotope production for Positron Emission Tomography (PET) imaging is equipped with an external beam line devoted to research activities in several fields such as detector physics, medical applications of particle physics, accelerator physics. Recently a widespread request has raised for the availability of well characterized proton and neutron beams, particularly for radiation hardness studies and the development of new neutron detectors. A feasibility study for a future upgrade of the Bern cyclotron towards a neutron facility was started, which requires a complete and precise characterization of the proton beam. Along this line, the measurement of fundamental parameters of the primary proton beam, such as the maximum proton energy and its spread have been performed by means of the RBS technique with two different targets, namely gold and graphite foils.

1. Introduction

The medical cyclotron facility at the Bern University Hospital is equipped with an IBA 18/18 Cyclone. It can accelerate H^- at the nominal energy of 18 MeV. The cyclotron is the central element of the SWAN enterprise, a combined project both for medical radioisotope production and research activities [1]. In particular, the night beam time is devoted at the production of ^{18}F , necessary for the synthesis of fluorodeoxyglucose to be used in PET imaging, while, during the day, different research activities are carried on, among which the production of new radioisotopes for medical applications [2], the development of new beam diagnostic apparatuses [3,4], and new detection techniques [5]. To make this possible, an external 6.5 m long Beam Transport Line (BTL) [6] was installed with two quadrupole doublets, two beam stoppers, a neutron shutter, a collimator and X/Y steerers. Recently, due to the increasing interest in the availability of well characterized neutron beams for several applications, among which neutron radiation hardness studies and tests

of new detectors [7–11], a project aiming at the implementation of a fully characterized neutron has been set up. In order to accurately select different neutron energies, it is fundamental to completely characterize the primary proton beam as well as the neutron production reactions and their cross-sections. Furthermore, the cyclotron beam characterization is crucial for the optimization of usual targets in medical routine and for the development of new techniques for radioisotope production. The two most relevant quantities to be assessed are the spatial profile and the energy distribution of the beam. In fact, beam profile measurements are important for optimizing the radioisotope production yield, while the precise knowledge of the beam energy distribution will determine both the target geometry (thickness) and cross-section calculations for the production of new radioisotopes. Recently, a system for online measurement of the transverse beam emittance and proton beam characterization was developed [4]. In this paper, we report on an alternative procedure for the absolute measurement of the energy of the protons accelerated by a medical cyclotron.

* Corresponding author at: Department of Physics “Ettore Pancini”, University of Naples Federico II, Complesso Universitario di Monte S. Angelo, Via Cintia, Napoli, Italy.

E-mail addresses: campajola@na.infn.it (L. Campajola), saverio.braccini@lhev.unibe.ch (S. Braccini), casolaro@na.infn.it (P. Casolaro), antonio.ereditato@lhev.unibe.ch (A. Ereditato), philipp.haeffner@lhev.unibe.ch (P.D. Häffner), paola.scampoli@unina.it (P. Scampoli).

<https://doi.org/10.1016/j.nimb.2018.12.017>

Received 10 October 2018; Received in revised form 5 December 2018; Accepted 6 December 2018

Available online 14 December 2018

0168-583X/ © 2018 Elsevier B.V. All rights reserved.

2. RBS method for energy measurement

The energy measurement has been performed by using the elemental analysis technique known as Rutherford Back-Scattering (RBS) [12–14]. When ions interact with a target in the energy range of \approx MeV, several physical processes take place, among which the elastic scattering. The back-scattered particles can be detected by a suitable particle detector and their residual energy determined. The analysis of the data is based on the application of the conservation principles of energy and momentum. At a given scattering angle θ (with respect to the beam axis), the energy of back-scattered particles (E_1) is a function of the energy of incident ions (E_0) and of the masses of projectiles and targets (M_1 and M_2 respectively):

$$E_1 = k(\theta, M_1, M_2) \cdot E_0 \quad (1)$$

The proportionality factor k takes the name of kinematic factor and it is given by:

$$k = \left[\frac{(M_2^2 - M_1^2 \sin^2 \theta)^{\frac{1}{2}} + M_1 \cos \theta}{M_1 + M_2} \right]^2 \quad (2)$$

The RBS technique is usually employed for the quantitative determination of the composition of a material and for depth profiling of elements. Reversing the problem, from the knowledge of the energy of backscattered particles, of the masses of the projectile, of the target nuclei, and of the detection angle, it is possible to determine the energy of the projectile as follows:

$$E_0 = \frac{E_1}{k(\theta, M_1, M_2)} \quad (3)$$

In this way, the measurement of the energy of backscattered protons from targets, with known composition, provides an accurate assessment of the incident beam energy.

3. Experimental setup

RBS measurements have been performed with the BTL by means of a scattering chamber that was specifically designed and built as shown in Fig. 1.

In such a scattering chamber, a target can be placed along the beam line and a totally depleted silicon detector can be positioned at the angle $\theta = 165.5^\circ$ ($\phi = 14.5^\circ$) for the detection of backscattered protons.

The scattering angle was chosen to reduce the rate on the detector due to the high proton beam intensity. Fig. 2 shows a schematic view of the chamber.

The proton beam interacts with the target positioned at the end of the chamber and backscattered protons are detected with the Si-detector with a 2 mm thick depleted region. Being the range of 18 MeV protons 1.99 mm in silicon, the backscattered protons are fully stopped inside the detector and their energy can be fully measured. Downstream of the target, the beam continues through a 70 cm long pipe ending with a Faraday Cup (FC). Such a long pipe prevents the detection of particles backscattered by the FC. In order to conveniently reduce the intensity of the beam and define a beam spot such to avoid proton diffusion from the chamber wall, a 2 mm diameter collimator was placed at the entrance of the chamber. The beam focusing was performed by maximizing the beam current on the FC. The silicon detector was preliminarily calibrated by means of a 10 kBq alpha source composed by a mixture of ^{241}Am and ^{239}Pu (5.15 and 5.48 MeV) and by means of additional energy points ranging from 1 to 20 MeV. These additional points were produced by means of a pulse generator (ORTEC, Model 419), providing signals with peak heights multiple and submultiple of a reference peak height, in our case that of the alpha source. Fig. 3 shows the calibration curve of the silicon detector.

The measurements of the cyclotron energy were carried out with two targets with different characteristic in terms of mass, atomic number and thickness. The first measurement was performed with a pure gold target whose thickness was 10 μm ; the second one with a graphite target of density 1.2 g/cm³ and a thickness of 75 μm .

4. Proton beam energy measurements

Fig. 4 shows the energy spectrum of the protons scattered by the gold target and detected at the angle $\theta = 165.5^\circ$. The experimental spectrum (black line) shows a main peak at the energy around 17.8 MeV. The gold target was positioned on a graphite frame causing the shoulder (or backscattering bulk) at energies below 13 MeV. The remaining part of the spectrum, not totally shown in Fig. 4, is mainly due to multiple scattering as well as to the electronic background.

Fig. 5 shows the energy spectrum of protons backscattered by the graphite target and detected at the same angle $\theta = 165.5^\circ$. The main peak at the energy of 13.08 MeV is due to protons backscattered by the graphite target.

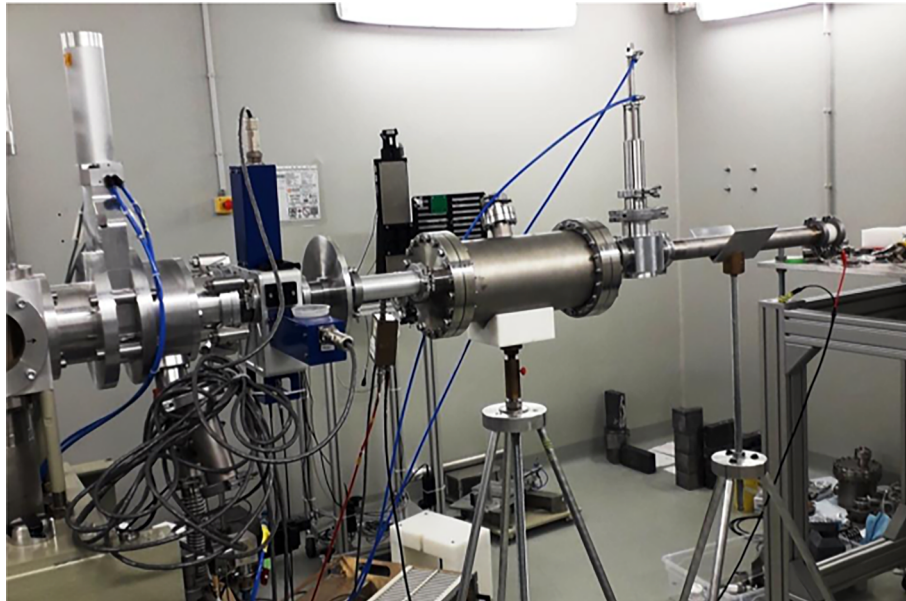


Fig. 1. The BTL of the Bern cyclotron with the scattering chamber for the energy measurement. The Faraday Cup (FC) is visible at the end of the beam line.

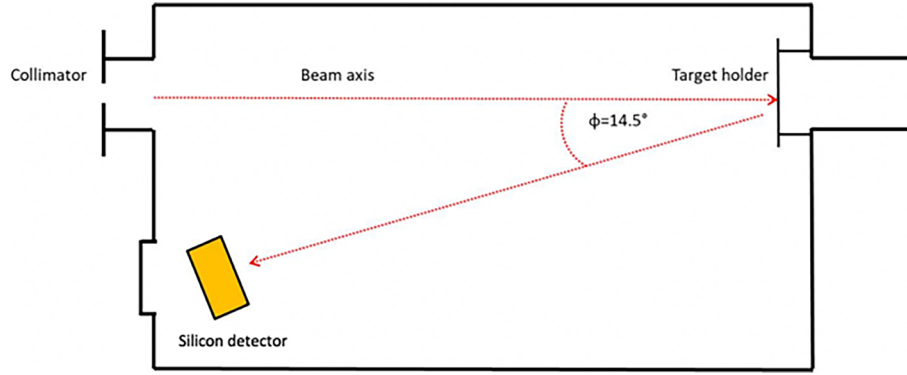


Fig. 2. Top view of the scattering chamber housing the target and the silicon detector.

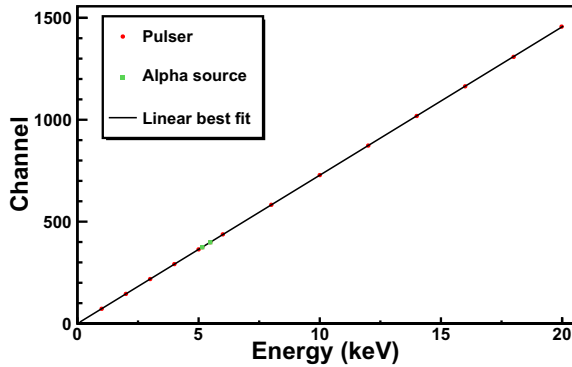


Fig. 3. Silicon detector calibration curve.

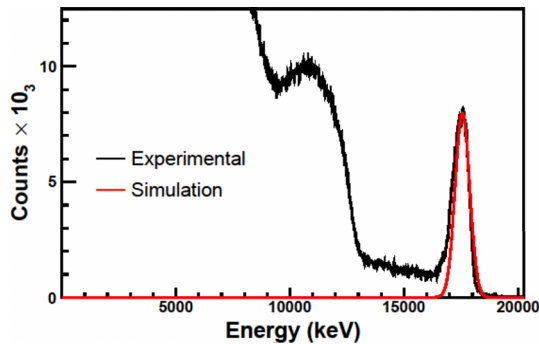


Fig. 4. Energy spectrum of protons backscattered on the gold target.

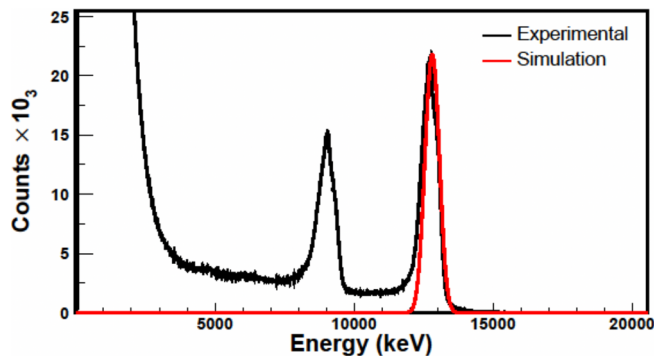


Fig. 5. Backscattered proton energy spectrum on the graphite target.

As in the case of the gold target, contributions are also present at low energies due to multiple scattering and electronic backgrounds. The second clear peak at the energy of 9.04 MeV arises from the first excited

Table 1

Results of the RBS analysis.

	Mass (a.m.u)	Target thickness (μm)	Kinematic factor	E_1 (MeV)	E_0 (MeV)
Gold	196.967	10	0.98020	17.84 ± 0.04	18.20 ± 0.04
Graphite	12.011	75	0.71898	13.08 ± 0.04	18.19 ± 0.05

state of the residual ^{12}C nuclei coming from the nuclear reaction $^{12}\text{C}(p, p')^{12}\text{C}^*$. The cyclotron energy was found to be as the middle point at half-height of the backscattering peak. The energy of the incident beam was calculated by means of Eq. (3) and the results are summarized in Table 1 for both targets.

The results of the two independent measurements are in excellent agreement. Furthermore, a Rutherford backscattering simulation was performed for the two target elements with the simulation program SIMNRA [13]. The same input parameters were used for gold and graphite. In particular, the incident proton energy was set to 18.19 MeV, the detector resolution to 40 keV and the energy spread of the incident beam to 0.51 MeV. SIMNRA results well agree with experimental data, as shown in Figs. 4 and 5 where simulated data are reported as a red line. The detector energy uncertainty, ΔE_{instr} , reported in Table 1 was quoted to be 40 keV. This uncertainty accounts for the detector resolution and electronic noise, while the propagation of statistical uncertainties is 40 keV for gold and 50 keV for graphite target. However, the overall energy spread ($\Delta E_{\text{overall}}$) of the Gaussian peaks in Figs. 5 and 6 was found to be 0.70 MeV and 0.69 MeV for gold and graphite, respectively. The assessment of the overall incident beam energy spread was performed by estimating the single contributions as follows:

$$(\Delta E_{\text{overall}})^2 = (\Delta E_{\text{instr}})^2 + (\Delta E_{\text{geom}})^2 + (\Delta E_{\text{RBS}})^2 + (\Delta E_{\text{beam}})^2 \quad (4)$$

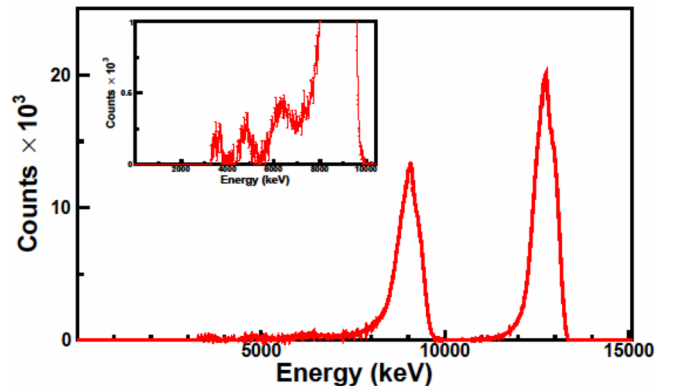


Fig. 6. Energy spectrum of backscattered proton on the graphite target after background subtraction. In the insert, a zoom at energies below 10 MeV.

Table 2

Contributions to the beam energy uncertainty.

	$\Delta E_{\text{overall}}$ (MeV)	ΔE_{instr} (MeV)	ΔE_{geom} (MeV)	ΔE_{RBS} (MeV)	ΔE_{beam} (MeV)
Gold	0.70	0.04	0.03	0.47	0.50
Graphite	0.69	0.04	0.03	0.47	0.51

Table 3Results of the analysis of ^{12}C excited levels.

NNDC ^{12}C E_{level} (MeV)	Q value (MeV)	E_{calc} (MeV)	E_{exp} (MeV)	ΔE (%)
0	0	12.78	12.74	−0.4
4.43891	−4.44	9.00	9.04	0.3
7.6542	−7.65	6.27	6.11	−2.8
9.641	−9.64	4.59	4.60	−0.1
10.3	−10.3	—	—	—
10.844	−10.84	3.56	3.56	0.1

ΔE_{instr} has already been defined above. ΔE_{geom} is the energy spread due to the detector geometrical acceptance and resulted to be 26 keV. The uncertainty on the θ angle was found to be negligible. ΔE_{RBS} is the energy spread due to the finite target thickness. In fact, protons lose their energy by interacting with the target atoms along the forward and backward paths. ΔE_{beam} is the energy spread of the incident beam. If the incident beam is orthogonal to the target surface, the ΔE_{RBS} can be estimated by means of the following formula:

$$\Delta E_{\text{overall}} = \left[k \left(\frac{dE}{dx} \right)_{E_0} + \frac{1}{\cos\theta} \left(\frac{dE}{dx} \right)_{kE_0} \right] \cdot t \quad (5)$$

where dE/dx is the stopping power [15] at energies E_0 and kE_0 , θ is the angle between the incident and scattering directions and t is the target thickness. The values of ΔE_{RBS} were estimated to be 0.47 MeV for both targets. The final evaluation of the incident energy spread ΔE_{beam} resulted to be 0.51 MeV (the average of the energy values for gold and graphite). The energy uncertainty contributions are summarized in Table 2.

As a further confirmation of the measured proton beam energy, the peaks corresponding to the excitation states of the ^{12}C atoms of the graphite due to the reaction $^{12}\text{C}(p, p')^{12}\text{C}^*$ were analysed. In Fig. 6 the energy spectrum of backscattered protons after background subtraction is shown.

The energy levels of the ^{12}C and the reaction Q-values evaluated from National Nuclear Data Centre (NNDC) database [16] are reported in Table 3 together with the calculated values of the peak energies (E_{calc}). In the last two columns of Table 3 the measured peak energy (E_{exp}) and the corresponding percent difference (ΔE) are reported. The agreement between theoretical and experimental data is excellent. Furthermore, the ^{12}C excited level with the energy of 10.3 MeV is not observed as it undergoes α -decay.

5. Conclusions

The measurement of the energy of the protons accelerated by the Bern cyclotron (IBA Cyclone 18/18) was successfully performed with the Rutherford backscattering analysis. Protons were scattered by two

different targets of pure gold and graphite and their residual energy measured at the angle $\theta = 165.5^\circ$ with a silicon detector. Knowing the composition of the targets, the incident energy was then inferred with the accuracy of 0.2%. The two measurements performed with two targets are in well agreement giving an energy of $E_0 = (18.19 \pm 0.05) \text{ MeV}$. Furthermore, the contribution to the overall uncertainty expressing the beam width was estimated to be $(\Delta E_{\text{beam}}) = 0.5 \text{ MeV}$. These results well agree with the further analysis performed on the excited states of the ^{12}C nuclei in the graphite target and with a previous measurement based on a different method [4]. The results presented in this paper will be instrumental for further developments, in particular for the implementation of a fully characterised neutron beam.

Acknowledgments

We acknowledge the contribution by the electronics and mechanics workshop of the Laboratory for High Energy Physics of the University of Bern. We also would like to thank Tommaso Stefano Carzaniga for his support during the measurement campaign and Mario Borriello for his technical contributions.

References

- [1] M. Auger, S. Braccini, A. Ereditato, M. Häberli, E. Kirillova, K. Nesteruk, P. Scampoli, Accelerator and detector physics at the Bern medical cyclotron and its beam transport line, *Nukleonika* 61 (1) (2016) 11–14, <https://doi.org/10.1515/nuka-2016-0009>.
- [2] T. Carzaniga, M. Auger, S. Braccini, M. Bunka, A. Ereditato, K. Nesteruk, P. Scampoli, A. Tärler, N. van der Meulen, Measurement of ^{43}Sc and ^{44}Sc production cross-section with an 18 MeV medical PET cyclotron, *Appl. Radiat. Isot.* 129 (2017) 96–102, <https://doi.org/10.1016/j.apradiso.2017.08.013>.
- [3] M. Auger, S. Braccini, T. Carzaniga, K. Nesteruk, P. Scampoli, A detector based on silica fibers for ion beam monitoring in a wide current range, *JINST* 11 (P03027) (2016) 0009, <https://doi.org/10.1088/1748-0221/11/03/P03027>.
- [4] K. Nesteruk, M. Auger, S. Braccini, T.S. Carzaniga, A. Ereditato, P. Scampoli, A system for online beam emittance measurements and proton beam characterization, *JINST* 13 (P03027). doi: <https://doi.org/10.1088/1748-0221/13/01/P01011>.
- [5] J. Anders, S. Braccini, T. Carzaniga, A. Ereditato, A. Fehr, F. Meloni, C. Merlassino, A. Miucci, M. Rimoldi, M. Weber, A facility for radiation hardness studies based on the Bern medical cyclotron, arXiv:1803.01939 [physics.ins-det].
- [6] S. Braccini, The new Bern PET cyclotron, its research beam line, and the development of an innovative beam monitor detector, *AIP Conf. Proc.* 1525 (P03027) (2013) 144–150, <https://doi.org/10.1088/1748-0221/13/01/P01011>.
- [7] A. Hands, et al., Single event effects in power MOSFETs due to atmospheric and thermal neutron, *IEEE Trans. Nucl. Sci.* 58 (6) (2011) 2687–2694.
- [8] C. Davidson, E.W. Blackmore, J. Hess, Failures of MOSFETs in terrestrial power electronics due to single event burnout, *IEEE INTELEC* (2004).
- [9] R. Nolte, J. Thomas, Failures of MOSFETs in terrestrial power electronics due to single event burnout, Monoenergetic fast neutron reference fields: II. Field characterization *Metrologia* (48.6) (2011) S274.
- [10] N. Zaitseva, et al., Recent developments in plastic scintillators with pulse shape discrimination, *Nucl. Instrum. Methods Phys. Res., Sect. A* 889 (2018) 97–104.
- [11] R. Bencardino, J. Eberhardt, Development of a fast-neutron detector with silicon photomultiplier readout, *IEEE Trans. Nucl. Sci.* 56 (3) (2009) 1129–1134.
- [12] P. Casolaro, L. Campajola, E. Balzano, R. Figari, E. Vardaci, G.L. Rana, Educational activities with a tandem accelerator, *Eur. J. Phys.* 39 (3) (2018) 035801.
- [13] M. Mayer, SIMNRA, a simulation program for the analysis of NRA, RBS and ERDA, *AIP Conference Proceedings* 475 (1).
- [14] K. Kimura, K. Oshima, M. Mammami, Monolayer analysis in Rutherford back-scattering spectroscopy, *Appl. Phys. Lett.* 64 (17) (1994) 2232–2234.
- [15] M. Berger, Stopping-Power and Range Tables for Electrons, Protons, and Helium Ions: Physical Reference Data, Physical Reference Data.
- [16] J. Tuli, Evaluated nuclear structure data file, *Nucl. Instrum. Methods Phys. Res., Sect. A* 369 (2) (1996) 506–511.